

Supporting Information for:

Intercorrelated ferroelectrics in 2D van der Waals materials

Yan Liang, Shiyong Shen, Baibiao Haung, Ying Dai,* Yandong Ma*

School of Physics, State Key Laboratory of Crystal Materials, Shandong University, Shandan Str.
27, Jinan 250100, People's Republic of China

*Corresponding author: daiy60@sina.com (Y.D.); yandong.ma@sdu.edu.cn (Y.M.)

COMPUTATIONAL METHOD

First-principles calculations. First-principles calculations are carried out based on density functional theory as implemented in the Vienna *Ab Initio* Simulation Package (VASP).¹ In which the exchange-correlation energy is modeled by the generalized gradient approximation (GGA) in the form of Perdew, Burke, and Ernzerhof (PBE).² The semi-empirical dispersion correction based on the DFT-D2 method of Grimme is employed to treat the interlayer vdW interactions.³ Convergence thresholds of 10^{-5} eV and 0.01 eV/Å are adopted, respectively, for energy and forces. A vacuum space larger than 18 Å is employed to eliminate the spurious interactions, and an energy cutoff of 500 eV is set. The ferroelectric polarization is computed by the Berry phase method.⁷ The energy barriers of ferroelectric switching are obtained by using nudged elastic band (NEB) method,⁴ and Berry curvatures are calculated by the maximally localized Wannier function method, as implanted in the Wannier90 code.⁵

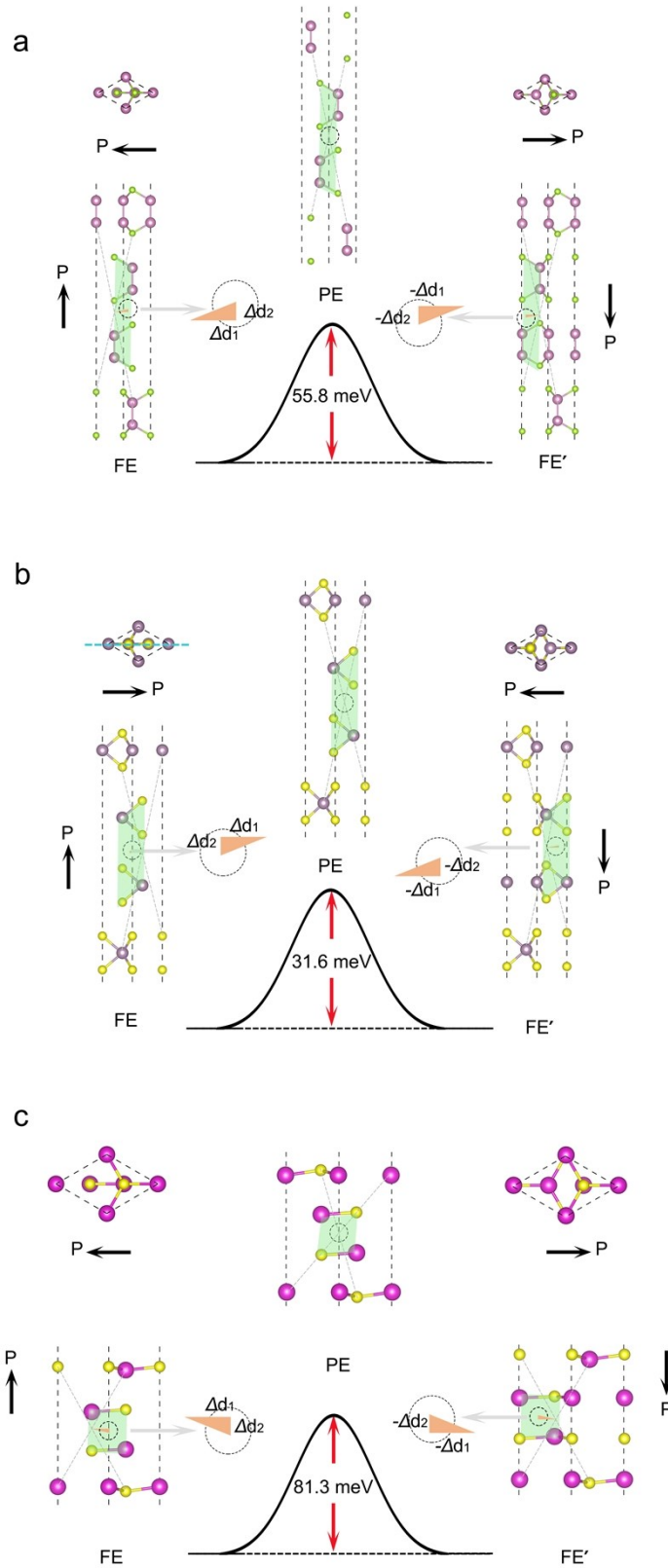


Figure S1. Minimum energy path for polarization reversal, along with the corresponding structures, of ABB'A' configuration of FL (a) InSe, (b) MoS₂ and (c) CdS.

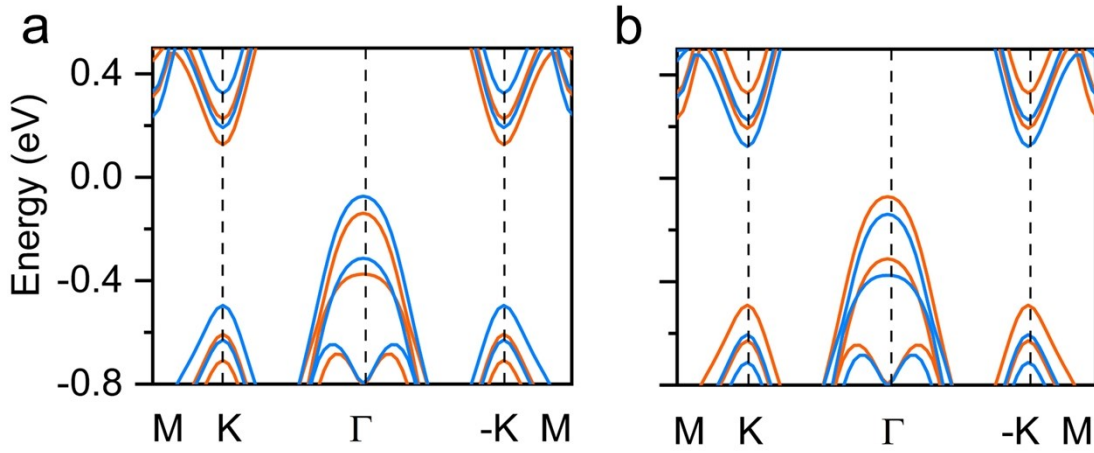


Figure S2. Band structures of FL VS₂ at FE and FE' states without SOC.

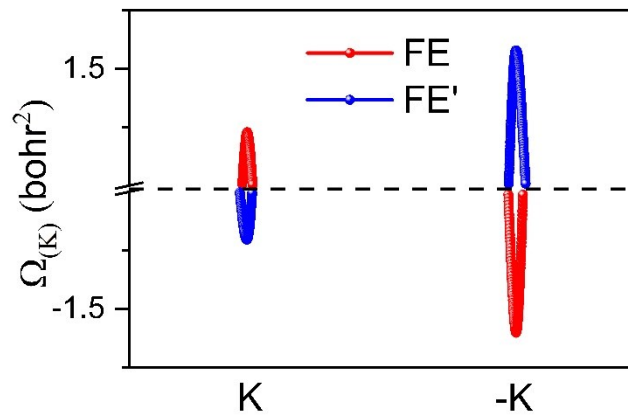


Figure S3. The out-of-plane Berry curvature $\Omega_{(k)}$ near the K and $-K$ for VS₂ FL at FE and FE' states.

When the 2D vdW multilayer with intercorrelated ferroelectrics are constructed by photovoltaic single layers, the bidirectional intrinsic electric field can facilitate the departure of photo-generated electrons and holes. Here, we take 2D photovoltaic material, CdS, as an example, and show the band structure as well as the corresponding partial charge densities of ABB'A' configuration FL CdS in **Figure S4**. It can be seen that the CBM and VBM are spatially separated to top and bottom layers, respectively. Hence, the lifetime of excitons and the photovoltaics' efficiency can be greatly enhanced.

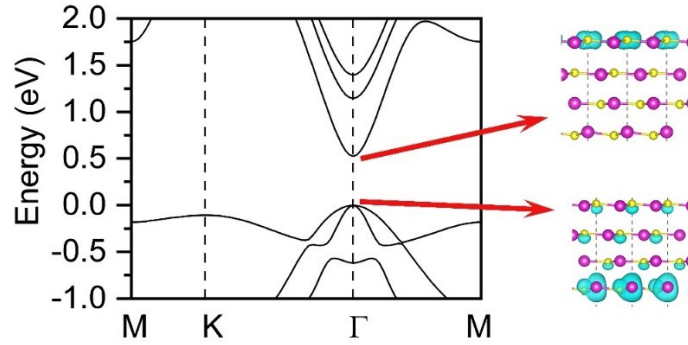


Figure S4. Electronic band structure and partial charge densities of CBM and VBM of ABB'A' configuration FL CdS.

Table S1. IP/OOP polarization (in e/cm^2) and energy barrier for ferroelectric switching (in meV/f.u.) of FL h-BN, FL InSe, FL MoS₂, FL CdS, TL PtSe₂, TL Bi₂Te₃, TL Ti₂CO₂ and TL Tl₂O. The FL (TL) systems are in the ABB'A' (AAB) configuration.

	BN	InSe	MoS ₂	CdS	PtSe ₂	Bi ₂ Te ₃	Ti ₂ CO ₂	Tl ₂ O
P _{OOP}	3.5×10^{12}	7.1×10^{10}	5.4×10^{11}	1.5×10^{13}	2.5×10^{11}	5.1×10^9	1.1×10^{11}	3.4×10^{10}
P _{IP}	1.9×10^{10}	9.4×10^9	7.7×10^9	9.3×10^{10}	1.6×10^{11}	3.1×10^{10}	3.5×10^9	2.3×10^{10}
E _b	15.6	55.8	31.6	83.1	63.7	34.9	34.4	33.1

The calculated moderate energy barriers imply the feasibility of their ferroelectric switching. Most systems exhibit a larger OOP polarization as compared with that of IP. While for TL Bi₂Te₃, the IP polarization is one magnitude larger than that of OOP. For TL PtSe₂ and Tl₂O, IP and OOP polarization values are comparable. These polarization values are comparable or even several order of magnitude larger than that of *d*1T MoTe₂ monolayer,^{6,7} h-BL⁸ and WTe₂ that have been detected in the experiments.^{9,10}

References

1. Kresse, G.; Joubert, D., From ultrasoft pseudopotentials to the projector augmented-wave method. *Phys. Rev. B* 1999, 59, 1758-1775.
2. Perdew, J. P.; Chevary, J. A.; Vosko, S. H.; Jackson, K. A.; Pederson, M. R.; Singh, D. J.; Fiolhais, C., Atoms, molecules, solids, and surfaces: Applications of the generalized gradient approximation for exchange and correlation. *Phys. Rev. B* 1992, 46, 6671-6687.
3. Grimme, S., Semiempirical GGA-type density functional constructed with a long-range dispersion correction. *J. Comput. Chem.* 2006, 27, 1787-1799.
4. Henkelman, G.; Uberuaga, B. P.; Jónsson, H., A climbing image nudged elastic band method for finding saddle points and minimum energy paths. *J. Chem. Phys.* 2000, 113, 9901-9904.
5. Marzari, N.; Mostofi, A. A.; Yates, J. R.; Souza, I.; Vanderbilt, D., Maximally localized Wannier functions: Theory and applications. *Rev. Mod. Phys.* 2012, 84, 1419-1475.
6. Yuan, S.; Luo, X.; Chan, H. L.; Xiao, C.; Dai, Y.; Xie, M.; Hao, J., Room-temperature ferroelectricity in MoTe₂ down to the atomic monolayer limit. *Nat. commun.* 2019, 10, 1775.
7. Bruyer, E.; Di Sante, D.; Barone, P.; Stroppa, A.; Whangbo, M.-H.; Picozzi, S., Possibility of combining ferroelectricity and Rashba-like spin splitting in monolayers of the 1T-type transition-metal dichalcogenides MX₂ (M=Mo,W;X=S,Se,Te). *Phys. Rev. B* 2016, 94, 195402.
8. Yasuda K, Wang X, Watanabe K, et al. Stacking-engineered ferroelectricity in bilayer boron nitride. *arXiv:2010.06600*, 2020.
9. Fei, Z.; Zhao, W.; Palomaki, T. A.; Sun, B.; Miller, M. K.; Zhao, Z.; Yan, J.; Xu, X.; Cobden, D. H., Ferroelectric switching of a two-dimensional metal. *Nature* 2018, 560, 336-339.
10. Yang, Q.; Wu, M.; Li, J., Origin of two-dimensional vertical ferroelectricity in WTe₂ bilayer and

multilayer. *J. Phys. Chem. Lett.* 2018, 9, 7160-7164.